Desalination and Water Treatment
www.deswater.com
doi: 10.5004/dwt.2020.25841

194 (2020) 235–247
August

Sequential process of electro-Fenton and adsorption for the treatment of gemstones dyeing wastewater

Thaís Strieder Machado[a], Bianca Carolina Ludwig[a], Igor Marafon Rodegheri[b], Kely Zambonin[c], Jonatan Rafael de Mello[d], Marcelo Hemkemeier[c], Guilherme Luiz Dotto[e], Jeferson Steffanello Piccin[a,*]

[a]*Postgraduate in Civil and Environmental Engineering, University of Passo Fundo, Campus I, BR 285, Zip Code: 99052–900, Passo Fundo, RS, Brazil, emails: jefersonpiccin@upf.br (J.S. Piccin), thaiis.strieder@hotmail.com (T.S. Machado), biancacarolinaludwig@gmail.com (B.C. Ludwig)*
[b]*Chemical Engineering Department, Federal University of São Carlos, Rod. Washington Luiz, Zip Code: 13565-905, São Carlos, SP, Brazil, email: marafigor@gmail.com (I.M. Rodegheri)*
[c]*Chemical Engineering Department, University of Passo Fundo, Campus I, BR 285, Zip Code: 99052–900, Passo Fundo, RS, Brazil, emails: kelyzambonin@gmail.com (K. Zambonin), marceloh@upf.br (M. Hemkemeier)*
[d]*Postgraduate in Food Science and Technology, University of Passo Fundo, Campus I, BR 285, Zip Code: 99052–900, Passo Fundo, RS, Brazil, email: mello.jonatan@gmail.com (J. Rafael de Mello)*
[e]*Chemical Engineering Department, Federal University of Santa Maria, Roraima Avenue, Zip Code: 97105–900, Santa Maria, RS, Brazil, email: guilherme_dotto@yahoo.com.br (G.L. Dotto)*

Received 11 September 2019; Accepted 16 March 2020

ABSTRACT

The processing of gemstones, mainly the dyeing step, generates a high volume of wastewater containing a high concentration of Rhodamine B. This wastewater is potentially toxic and contains non-biodegradable substances. For this reason, it is necessary to develop methodologies to treat this type of wastewater. Therefore, in this work, a sequential process of electro-Fenton conjugated with adsorption were developed to treat this type of wastewater. The gemstones dyeing wastewater presented between 735.5 and 1,943.0 mg L^{-1} of Rhodamine B. Firstly, the electro-Fenton process was applied, and removal superior to 65% of the RhB concentration were observed. Subsequently, adsorption was applied using a strong cationic resin at a pH of 2.0. In this condition, the adsorption capacity predicted by the Langmuir model was 247.3 mg g^{-1}. The breakthrough curves were inclined with a suitable mass transfer zone. The sequential process of electro-Fenton and fixed-bed adsorption were able to remove 100% of the RhB from the gemstones' wastewater, being an effective alternative to treat this type of effluent.

Keywords: Advanced oxidative process; Agate dyeing; Ion-exchange; Non-conventional treatment; Real wastewater

1. Introduction

In the gemstones' industry, the process of dyeing is performed to aggregate commercial value, and it is realized in basically every produced and commercialized gem. To achieve the colors red and pink, the gems are immersed in solutions containing alcohol and Rhodamine B dye (RhB). After few days, the gems are washed, producing approximately 20 L of wastewater per kg of colored gem. The concentrated color and the non-degradable nature of

* Corresponding author.

this wastewater constitute serious environmental issues [1]. Normally, physical, physicochemical, and chemical oxidation with sodium hypochlorite are applied in the treatment of wastewater from gemstones. These processes have the inconvenience of generating a large volume of sludge with dangerous characteristics and is associated with the formation of chlorinated compounds in effluents [2]. Moreover, the recalcitrant effect of dyes and no-completely mineralized substances cause a reduction in efficiency of wastewater conventional biological treatment systems [3]. In this way, many studies have been carried out to propose solutions to the treatment of effluents containing dyes. For the removal of RhB, it can be mentioned, for example, adsorption [4], sonication [5], electrolysis, including electro-Fenton [6], photocatalysis [7], membrane separation process [8], and ionic exchange [9]. However, the majority of these papers presented in literature have been done with synthetic aqueous solutions and/or low RhB concentrations. So, it is difficult to apply in real gemstones effluents, where, there are other compounds, including salts, ethanol and detergents [3], and RhB is highly concentrated.

Advanced oxidative processes are an effective alternative in the degradation of effluents with toxic fillers, including dyes like RhB. They have characteristics that make them clean technology due to the non-generation of sludge or phase transfer of the pollutant [10]. The technology is based on the generation of free radicals, especially the hydroxyl radical (*OH) of high oxidizing power. One way to generate the hydroxyl radical is through the Fenton reaction. It uses hydrogen peroxide (H_2O_2) in the presence of catalysts, including O_3, UV radiation, and iron salts [11]. In the electro-Fenton process, the H_2O_2 generation occurs by the hydrolysis of water in dissolved oxygen medium. Alternatively, the production of iron may be due to the decomposition of the anode. These reactions are demonstrated according to Eqs. (1) and (2), respectively [6].

$$O^2_{(g)} + 2H^+_{(aq)} + 2e^- \rightarrow H_2O_{2(aq)} \quad (1)$$

$$Fe^0_{(s)} - 2e^- \rightarrow Fe^{2+}_{(aq)} \quad (2)$$

One of the problems with the electro-Fenton process is the energy cost of pollutant degradation, especially at low concentrations. For example, Nidheesh and Gandhimathi [12] verified an energy consumption of approximately 50 kWh per kg of removed RhB of a 50 mg L^{-1} aqueous solution. Moreover, in several cases, the removal of pollutants from effluents after advanced oxidation processes was not completely, with the need for complementary treatment methods [13]. For these reasons, recent works have used the adsorption coupled to the electro-Fenton process to complementary removal of dyes and other substances [13–16].

Adsorption is one of the most effective methods for the removal of water-soluble substances, even at low concentrations. Low energy requirement, the absence of by-products with greater toxicity, and the capacity of regeneration of adsorbents are considerable attractive in its favor. It is applied to remove dyes present in the water of different industries, including textile [17], pulp and paper [18], tannery [19], and food industries [20]. For the correct analysis and scaling of the adsorption system, the determination of equilibrium curves and adsorption dynamics in fixed bed is necessary [21]. The recent literature reports few studies with electro-Fenton and adsorption, used individually or conjugated, for the removal of dyes present in real wastewater. Most studies use aqueous solutions and usually at concentrations much lower than those observed in real wastewater.

Therefore, the present work aims to propose an efficient, economically and environmentally sustainable process for the treatment of effluents containing Rhodamine B (a sequential process of electro-Fenton and adsorption), in particular of the dyeing of semi-precious stones. For this purpose, the treatment of real gemstones dyeing wastewater was firstly performed using electro-Fenton process, where the conditions were optimized by multi-response surface methodology. Subsequently, adsorption was applied. For the adsorption study, different adsorbent materials were evaluated, equilibrium curves were constructed and dynamic tests in fixed bed column were performed.

2. Materials and methods

2.1. Collection and characterization of gemstones dyeing wastewater

The wastewater samples, containing the dye RhB, from the gemstones processing were supplied by a company located in the north region of Rio Grande do Sul, Brazil. Three samples were collected from the agate wash step after they were dyed. The wastewater from the first sample was used to experimental execution of this work. The wastewater characteristics and characterization methods are presented in Table 1. RhB concentrations were determined by spectrophotometry at 554 nm [6]. Other characterization methods were performed according to the Standard Methods for the examination of water and wastewater [22].

2.2. Electro-Fenton process

The electrolytic system was composed of a cylindrical reactor 85 mm of diameter and 150 mm height (working volume of 500 mL). A pair of electrodes, a commercial steel cathode and titanium coated with ruthenium oxide (Ti/RuO_2) anode (De Nora, Brazil), were arranged vertically and distally at 10 mm. The projected area of the anode was 0.001182 m^2. The electric current supply was realized under galvanostatic conditions (constant current) through a source of continuous current (Dawer, FSCC 5002D). Between the electrodes, air was injected at a flow rate of 0.3 L min^{-1}.

Electro-Fenton (EF) process was evaluated using a response surface methodology using a central composite design (CCD) [23]. The variables evaluated were the current density (X_1), pH (X_2), and Fe^{2+}concentration (X_3) on the removal of RhB (R, Eq. (3)) and specific energy cost (CE, Eq. (4)). The real and coded levels of the CCD are described in Table 2 (in the Results section). The pH of the wastewater was adjusted using HCl or NaOH (0.1 mol L^{-1}). Fe^{2+} was added to wastewater from a 100 mg L^{-1} solution of Fe_2SO_4. Experimental conditions were defined according to the

Table 1
Physical–chemical characterization of gemstone wastewater containing RhB

Parameter	First sample[a,b]	Second sample[a]	Third sample[a]	Method
COD (mg L^{-1})	10,113.0 ± 597.8	13,280.0 ± 60.7	5,511.1 ± 155.3	5,220[d]
pH	3.30 ± 0.01	2.08 ± 0.01	3.24 ± 0.03	4,500[d]
RhB concentration (mg L^{-1})	1,943.0 ± 46.5	1,793.3 ± 30.3	735.5 ± 2.8	Spectrophotometry at 554 nm[c]
Turbidity (NTU)	35,000 ± 264	49,733 ± 901	38,150 ± 1,420	2,130[d]
Color (hazen)	2,693.0 ± 116.6	3,200.0 ± 200.0	3,703.3 ± 116.7	2,120[d]

[a]Mean ± standard deviation, $n = 3$; [b]Sample used in the experiments; [c]Tian et al. [6]; [d]APHA [22].

Table 2
Design matrix of CCD for current density (X_1), pH (X_2), and Fe^{2+} concentration (X_3) and observed responses to RhB removal (R, in %) and specific energy consumption (CE, in kWh kg^{-1})[a]

Experiment	X_1 (J in A m^{-2})	X_2 (pH)	X_3 ([Fe^{2+}] in g L^{-1})	R (%)	CE (kWh kg^{-1})
1	–1 (100)	–1 (2.0)	–1 (1.0)	66.31	1.64
2	+1 (150)	–1 (2.0)	–1 (1.0)	64.73	2.98
3	–1 (100)	+1 (3.0)	–1 (1.0)	54.07	2.81
4	+1 (150)	+1 (3.0)	–1 (1.0)	58.59	4.84
5	–1 (100)	–1 (2.0)	+1 (1.5)	60.78	1.95
6	+1 (150)	–1 (2.0)	+1 (1.5)	63.45	3.59
7	–1 (100)	+1 (3.0)	+1 (1.5)	56.79	2.33
8	+1 (150)	+1 (3.0)	+1 (1.5)	49.08	5.02
9	0 (125)	0 (2.5)	0 (1.25)	58.81	2.82
10	0 (125)	0 (2.5)	0 (1.25)	56.82	2.68
11	0 (125)	0 (2.5)	0 (1.25)	56.89	2.91
12	–1.68 (83)	0 (2.5)	0 (1.25)	53.12	2.19
13	+1.68 (167)	0 (2.5)	0 (1.25)	60.25	5.81
14	0 (125)	–1.68 (1.66)	0 (1.25)	61.21	1.86
15	0 (125)	+1.68 (3.34)	0 (1.25)	46.22	5.72
16	0 (125)	0 (2.5)	–1.68 (0.83)	55.14	3.33
17	0 (125)	0 (2.5)	+1.68 (1.67)	57.80	3.01

[a]$[RhB]_0 = 1{,}793.3 \pm 30.3$ mg L^{-1}; The values given in parentheses are the experimental conditions used in each experiment.

literature [12,24] and preliminary experiments (data not shown).

$$R = \frac{\left(C_0 - C_f\right)}{C_0} \times 100 \tag{3}$$

$$\mathrm{CE} = \frac{\int i \cdot V \cdot dt}{\left(C_0 - C_f\right) \cdot V_t} \tag{4}$$

where C_0 and C_f are the initial and final chemical oxygen demand (COD) concentration (kg m^{-3}), i is the current intensity (A), V is current tension (V), and V_t is the effluent treated volume (m^3). The integral of Eq. (2) was graphically solved considering measurements of i and V at intervals of 5 min [25].

The responses (R and CE) were evaluated using variance analysis (ANOVA) using an F-Fisher test, relating the variance of treatments and the variance experimental. The null hypothesis was rejected when the probability of type I error was inferior to 15% [26]. Operations conditions were determined by multi-response optimization using Derringer desirability function, according to Montgomery [23].

2.3. Adsorption experiments

Adsorption experiments were performed in three different stages, using the effluent treated by the optimized conditions of the electro-Fenton process and an aqueous solution containing only RhB dye (analytical degrees, Vetec) in the same concentration that electro-Fenton effluent.

- Initially the effect of pH 2–9 on the adsorption capacity of three different commercial adsorbents (activated carbon (Vetec, Brazil), strongly acidic ion exchange resin (Purolite, SSTPPC60H, Netherlands), and weak basic acidic ion exchange resin (Purolite, PPA100Plus) was

verified. For this, the pH of 50 mL of electro-Fenton effluent was corrected with HCl 0.1 mol L^{-1} and NaOH 0.1 mol L^{-1} and added to 0.25 g of each adsorbent (in the case of SA resin are used 0.05 g). The flasks were agitated in an orbital shaker (Tecnal, TE421, Brazil) at 25°C and 100 rpm for 24 h. After this, RhB concentration was determined in the liquid phase and expressed in adsorption capacity according to Eq. (5).

$$q = \frac{\left(C_0 - C_f\right)V}{w} \tag{5}$$

where C_0 and C_f are the initial and final concentration of RhB in the liquid phase (mg L^{-1}), V is the solution volume (L) and w is the mass of adsorbent (g).

- Subsequently, the equilibrium adsorption isotherms were obtained for the adsorbent and pH selected in the previous step. These steps were performed with the effluent containing RhB previously treated by electro-Fenton process and, in parallel, with synthetic aqueous solutions. The equilibrium adsorption were performed by batch experiments. The adsorbent material (0.05–0.5 g, dry basis) was added to 50 mL of RhB solutions (real or synthetic) and the system was stirred in an orbital shaker at 100 rpm and 25°C. The samples were analyzed after 24 h interval and equilibrium was reached when the liquid phase dye concentration showed a variation coefficient inferior to 5% in three consecutive measures [27]. The adsorption capacity (q_e) was determined by Eq. (5), for final concentration change to equilibrium concentration.
- Lastly, the breakthrough curves were obtained through a fixed bed column built-in stainless steel, with an internal diameter of 25 mm and length of 50 mm, attached to an infusion pump (Braun brand, Infusomat, Germany). The RhB solutions were poured in the upward direction through the adsorbent bed at 5, 10, and 15 mL min^{-1}. The outlet RhB concentration (C_t) was verified in gaps between 5 and 30 min, as needed, being expressed in relation to the initial concentration (C_0) as a time function. The breakthrough time (t_b) was defined as the concentration of the column output was greater than 1% of the input concentration value (C_t/C_0 = 0.01). Length of unused bed (LUB) and volume of treated effluent (V_b) are calculated according to Eqs. (6) and (7):

$$\text{LUB} = \left(1 - \frac{t_b}{t_e}\right)L \tag{6}$$

$$V_b = t_b Q \tag{7}$$

where t_e is the exhaustion time (at C_t/C_0 = 1, in min), L is the bed length (0.05 m), and Q is the flow rate (L min^{-1}).

After, defining the conditions of operation in a fixed bed an experiment was carried out increasing the bed length to 300 mm. The experiment was conducted to the breaking point. The effluent was collected and characterized for comparison with the gemstones' wastewater.

2.4. Data analysis of the adsorption isotherms and breakthrough curves

The equilibrium data were compared to the Langmuir and Freundlich isotherm models [27], according to Eqs. (8) and (9), respectively:

$$q_e = \frac{q_m k_L C_e}{1 + k_L C_e} \tag{8}$$

$$q_e = k_F C_e^{\frac{1}{n}} \tag{9}$$

where q_e is the adsorption capacity at equilibrium (mg g^{-1}), C_e is the equilibrium concentration at the liquid phase (mg L^{-1}), q_m is the maximum adsorption capacity (mg g^{-1}), n (dimensionless) is the heterogeneity factor, k_L (L mg^{-1}) and k_F ($mg^{(n-1)/n}$ $L^{1/n}g^{-1}$) are the constants of the Langmuir and Freundlich models, respectively.

The breakthrough curves were correlated to the Thomas and Wolborska models [28], according to Eqs. (10) and (11):

$$\frac{C_t}{C_0} = \frac{1}{1 + \exp\left(\frac{k_{\text{Th}} q_0 w}{Q} - k_{\text{Th}} C_0 t\right)} \tag{10}$$

$$\frac{C_t}{C_0} = \exp\left(\frac{k_w C_0}{q_0} t - \frac{k_w z}{v_z}\right) \tag{11}$$

where C_0 and C_t (mg L^{-1}) are the feed and outlet RhB concentrations of the column in any time, respectively, w the mass of adsorbent (g), Q the operation flow (L min^{-1}), k_{Th} and k_w are the kinetic constant of the Thomas and Wolborska models (L mg^{-1} min^{-1}), q_0 the stoichiometric capacity of the bed (mg g^{-1}), z is the bed length (m) and v_z is the interstitial velocity (m min^{-1}), and t the operation time at which the sample was retrieved (min).

For the model adjust to the experimental data it was utilized the software Matlab® and computational algorithms available at supplementary material 1. The model adjust quality was checked through the determination coefficient (R^2) and average relative error (E).

3. Results and discussion

3.1. Electro-Fenton process optimization

Table 2 presents the matrix of the central composite design and the responses of each experiment. The highest removal of RhB and the lowest energy cost of treatment, corresponding to 66.31% at 1.64 kWh kg^{-1}, respectively, were observed under conditions of 100 A m^{-2}, pH 2.0, and 1.0 g L^{-1} of Fe^{2+}, corresponding to experiment 1.

Statistical analysis (Tables S2.1 to S2.3 and in the Fig. S2.1 in the supplementary material 2) showed that for the removal only the linear effect of pH was significant. This demonstrates that other conditions applied are adequately optimized for the removal of RhB. However, the linear and negative effects of pH demonstrate that its decrease causes an increase of

RhB removal. Thus, is impossible to determine optimal conditions for this response in the study region.

For the energy cost of treatment, in order of magnitude, the significant effects on the response were J (X_1) > pH (X_2) > J^2 (X_1^2) > pH^2 (X_2^2) > J × pH ($X_1 \times X_2$). In both cases, the linear, quadratic, or interaction effects of Fe^{2+} (X_3) were not significant. The optimum operating conditions for this response are 90.2 A m^{-2} and pH 2.0. From the ANOVA, the non-significant effects on the responses were taken from the statistical models, and the removal (R) and energy cost of treatment (CE) were represented by Eqs. (12) and (13), respectively. Fig. 1 shows the response surface for the energy cost of treatment.

$$R(\%) = 57.6 - 4.54X_2 \tag{12}$$

$$\mathrm{CE}\left(\mathrm{kWh\,kg^{-1}}\right) = 2.85 + 1.01X_1 + 0.29X_1^2 + 0.83X_2 + 0.22X_2^2 + 0.22X_1X_2 \tag{13}$$

The pH exerts one of the main effects on electro-Fenton processes. In acid media, the production of H_2O_2 is high [29]. In addition, pH affects the iron speciation in solution, including the formation of Fe^{3+}, $Fe(OH)^{2+}$, and $Fe(OH)_2^{4+}$ species at basic pH, and altering the solubility of the species in solution [12]. For this reason, the increase in pH causes iron species to start precipitating in the form of iron hydroxide, negatively affecting the concentration of the hydroxyl radical (OH^-).

The current intensity (J) is the force that drives the reduction of oxygen to the formation of hydrogen peroxide at the cathode. The attraction force of the RhB toward the cathode also increases with the increase of the applied current, provoking a greater frequency of collision between the hydroxyl radical [12]. However, the increase of the current intensity applied can decrease the efficiency of removal of RhB, due to the formation of H_2O_2 by the reduction of oxygen protons, leading to less formation of hydrogen peroxide [30]. In addition, the increase in current intensity leads to higher energy consumption, increasing the cost of effluent treatment.

In relation, the effect of the concentration of Fe^{2+} added in the solution is due to the fact that its acts as an electron donor for the formation of the hydroxyl radical [31,32]. In conventional Fenton processes, the ratio of iron ferric species is 5–15 parts per part of H_2O_2 [12,27]. In electro-Fenton processes, where the oxidizing agent (H_2O_2) must be produced in situ, the optimization of Fe^{2+} concentration must be adequately performed. The fact that this effect does not appear significant on both responses shows that in the concentrations used are in sufficient quantity for the removal of RhB.

The multi-response optimization of the electro-Fenton process was performed (according to Fig. 2 in Supplementary material 2). The conditions were optimized for a current density of 110 A m^{-2}, pH 2, and [Fe2+] of 1 g L^{-1}. The predicted values for this condition were 62.8% of RhB removal and a treatment energy consumption of 1.805 kWh kg^{-1}. To verify the reproducibility of the electro-Fenton system in the treatment of gemstones dyeing wastewater, the other samples collection (sample 2 with 1,793.3 mg L^{-1} and sample 3 with 735.5 mg L^{-1} RhB) were subjected to treatment under the optimized condition.

Fig. 2 show that the removal of RhB was higher for the wastewater with the lowest initial dye concentration. The opposite was observed for energy consumption, indicating that the electro-Fenton process is economically disadvantageous when the dye concentration is low. As an example of this behavior, the energy consumption of 50 kWh kg^{-1} for the removal of 98% RhB in a 50 mg L^{-1} aqueous dye solution [12]. In addition, during RhB degradation, lower molecular weight sub-compounds may be produced due to incomplete mineralization, including phenols, linear, and branched hydrocarbons, diethyl amines, and nitrogenated phenol [12,33]. For this reason, the electro-Fenton process was conducted until the effluent concentration was around 500 mg L^{-1}. If this effluent is discharged into a receiving body, it may cause a significant change in color,

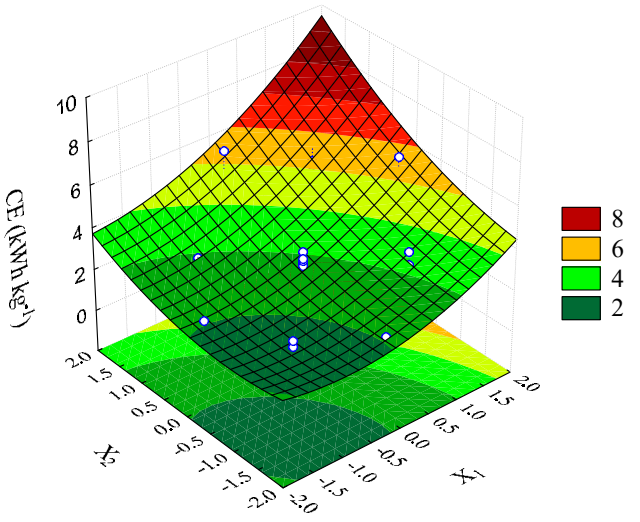

Fig. 1. Response surface of specific energy cost (CE) of RhB removal in the function of current density (X_1) and pH (X_2) ([Fe^{2+}] = 1 g L^{-1}).

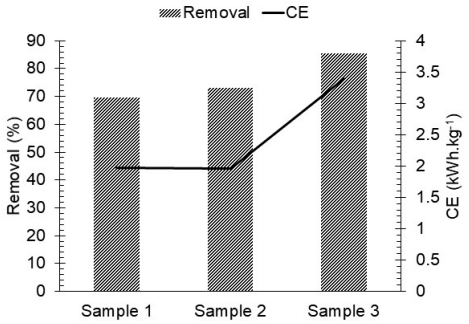

Fig. 2. Application of the optimized electro-Fenton process (110 A m^{-2}, pH = 2.0, and [Fe^{2+}] = 1 g L^{-1}) in different wastewater samples of gemstones dyeing wastewater (sample 1: $[RhB]_0$ = 1,943.0 mg L^{-1}; sample 2: $[RhB]_0$ = 1,793.3 mg L^{-1}; sample 3: $[RhB]_0$ = 735.5 mg L^{-1}).

contrary to local legislation to wastewater disposition [34]. Therefore, subsequent to the electro-Fenton process, adsorption was used as a complementary treatment technique as it was able to remove contaminants even at low concentrations such as milligrams or micrograms per liter [28].

3.2. Adsorption process

3.2.1. Effects of pH and adsorbent type on the RhB removal

Fig. 4 shows the effect of the pH over the RhB adsorption in dyeing wastewater of gemstones. It is observed that strongly acidic resin, followed by the active carbon, possess the highest adsorption capacity. With the pH increase, the adsorption capacity of strongly acid resin decrease of approximately 150 mg g^{-1} (pH 2) to 50 mg g^{-1} (pH 4). Thus, is observed that in low acid, neutral or basic conditions acid resin presented adsorption capacity similar at commercial activated carbon. The poor adsorption capacity of anionic resin shows that there is no interaction between it and the adsorbent.

According to Fig. 3, there was an increase in the strongly acidic resin adsorption capacity with the pH reduction explained by the increase of number of H^+ protons in the aqueous solution under acid conditions. Additionally, with the RhB dissociated in cations with positive charges, that attract the partials negative charges of resin sulfonic groups, through electrostatic interactions [35,36]. In addition, the cationic character of the strong acid resin, characterized by the $R–SO^{3-}$ grouping, it's able to interact electrostatically with RhB degradation sub-compounds during the electro-Fenton process. This way, at pH 2, it was observed the highest RhB removal capacity in gemstones dyeing wastewater, being this the adopted condition at the following experiments.

3.2.2. Adsorption isotherms

The results of the adsorption equilibrium at pH 2 and temperature at 25°C by the strongly acidic resin in contact with the real and aqueous solution for RhB are presented in Fig. 4. The equilibrium was reached after 2 d of contact.

Fig. 4 shows that according to the classification suggested by Giles et al. [37], the RhB adsorption isotherms by strongly acidic resin present the H2 class, where the RhB molecules have high affinity with the adsorbent surface. This way, the initial amount adsorbed is high even with low RhB concentrations in the mean. In addition, this type of isotherm is characterized by the formation of a plateau with maximum adsorption capacity, characteristic of the formation of a single layer of the adsorbate over the adsorbent [27].

Furthermore, it is observed that comparing the equilibrium curve of the real wastewater with the RhB aqueous solution on the same conditions, the adsorption capacities are similar, showing that the compounds used during the dyeing or washing of the gemstones do not affect importantly the adsorption process. Differently, several studies have shown inferior adsorption capacities in real wastewater to that observed in aqueous solutions, due to competition for adsorption sites [38,39], which suggests affinity for the selective removal of the RhB.

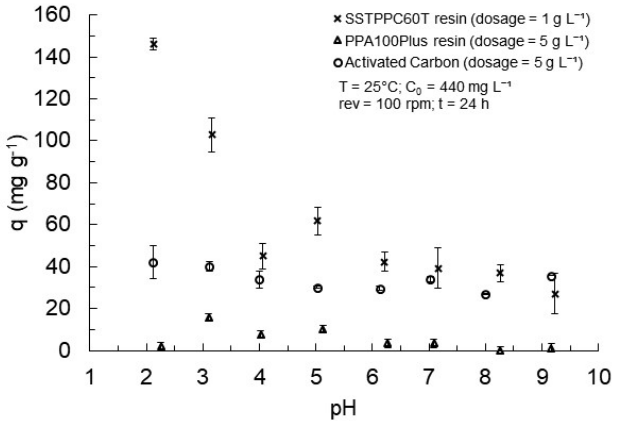

Fig. 3. Effect of the pH in the RhB adsorption (real gemstones' wastewater treated by electro-Fenton) by weak basic resin (PPA100Plus), strongly acidic resin (SSTPPC60T), and activated carbon.

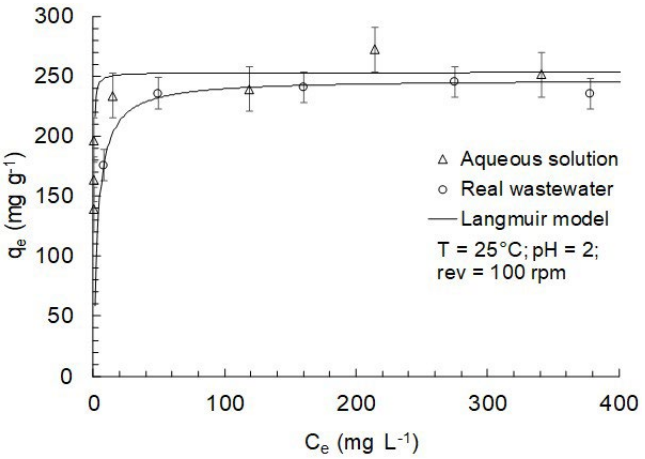

Fig. 4. Adsorption isotherms of RhB (aqueous solution and real gemstones' wastewater treated by electro-Fenton) by strongly acidic resin.

Table 3 presents the parameters of Langmuir and Freundlich models that adjust to the equilibrium data of the RhB adsorption. The theoretical models indicate better adjust to the Langmuir model to the equilibrium data (solid lines in the Fig. 4), because it presents the determination coefficient ($R^2 > 0{,}90$) and low medium relative error ($E \leq 10\%$). This confirms the coverage in a single-layer of the RhB in the cationic resin [35].

In relation to the Langmuir model parameters, it is observed a denser coverage of the single-layer by the RhB relative to the real wastewater. Nonetheless, verifying the thermodynamic coefficient of the Langmuir model (k_L) of the real wastewater, were better than the simulated wastewater, and indicate that the Langmuir model is capable of predicting the experimental data of the cationic resin equilibrium, when in contact with the real wastewater.

Other authors reported that experimental data have adjusted to the Langmuir model in the RhB adsorption by conventional or alternative adsorbents. Anandkumar and

Table 3
Parameters of Langmuir and Freundlich models for adsorption isotherm of RhB by strongly acid resin

Parameter	Real wastewater	Aqueous solution
	Langmuir	
k_L (L mg^{-1})	0.307	5.920
q_m (mg g^{-1})	247.30	253.13
R^2	0.991	0.902
E (%)	1.03	6.41
	Freundlich	
k_F (mg$^{(n-1)/n}$ L$^{1/n}$g^{-1})	162.02	178.86
N	13.10	14.41
R^2	0.798	0.860
E (%)	4.62	7.64

T = 25°C; pH = 2.0

Mandal [40] observed that tannery residual biomass obtained from the vegetable tanning process has the RhB adsorption capacity of 212.77 mg g^{-1}. This value is lower than observed by Huang et al. [41], which uses an activated carbon developed from *Lythrum salicaria* L. modified with pyruvic acid, with an adsorption capacity of 370.37 mg g^{-1}. However, other authors have reported RhB adsorption capacities in the order of units and tens of mg g^{-1} [42,43].

3.2.3. Breakthrough curves

Fig. 5 shows the breakthrough curves of the wastewater adjusted to the electro-Fenton process final concentration. Column was composed with 15 g of strongly acidic resin, with a bed length of 5 cm. The results regarding model parameters of breakthrough are shown in Table 4.

According to Fig. 5, it is observed that flow increase has managed the bed to saturate faster. As it can be observed, to the 5 mL min^{-1} flow (for real wastewater) the concentration begins to increase from 66 min on (breakthrough time). In 465 min, the adsorbate concentration in the column outlet reaches close to the feed, indicating the exhaustion of the bed. The comparison of the breakthrough curves of the real wastewater and the aqueous solution (at a flow rate of 5 mL min^{-1}) show similar results of breakthrough time. However, lower slope behavior, causing an increase of exhaustion time and the LUB.

For the breakthrough curves at 10 and 15 mL min^{-1} as soon as the first instants the concentration already starts to increase, and the exhaustion of bed occurs at 165 and 100 min, respectively. Moreover, the LUB increase and the volume of treated effluent decrease with the increase of flow rate. The decrease of breakthrough time with the flow rate increase is observed by Ghribi and Bagane [44] to RhB adsorption on natural clay.

The feed rate of the bed increases the amount of solute to be adsorbed in a particular intrusion. Therefore, a higher saturation of the bed is expected at higher flows. In the other hand, the increase in feed flow influences directly the external mass transfer, facilitating the adsorption on the surface of the material. Similar results were observed by Canteli et al. [45] and El-Naas et al. [46].

Table 4
Experimental results and parameters of Thomas and Wolborska models for breakthrough curves of RhB by strongly acid resin

Parameter	Flow rate (mL min^{-1})			
	5	10	15	5[a]
t_b (min)	66.1	12.8	9.4	67.8
t_e (min)	465	165	100	800
LUB (m)	0.043	0.046	0.045	0.046
V_b (L)	0.330	0.064	0.047	0.339
Thomas model				
$k_T \times 10^5$ (L (mg min)$^{-1}$)	4.10	8.90	17.4	2.53
q_0 (mg g^{-1})	32.48	25.34	18.73	35.00
R^2	0.989	0.976	0.988	0.992
Wolborska model				
$k_w \times 10^5$ (L (mg min)$^{-1}$)	0.84	2.40	3.68	0.54 × 10^{-5}
q_0 (mg g^{-1})	64.73	52.09	41.57	105.08
R^2	0.793	0.836	0.802	0.834
q_e (mg g^{-1})[b]	257.74	257.74	257.74	253.09

[a]Aqueous solution contains RhB; [b]experimental value predicted by Langmuir isotherm; pH = 2.0; T = 25°C; C_0 = 483.9 mg L^{-1}; z = 5 cm; w = 15 g.

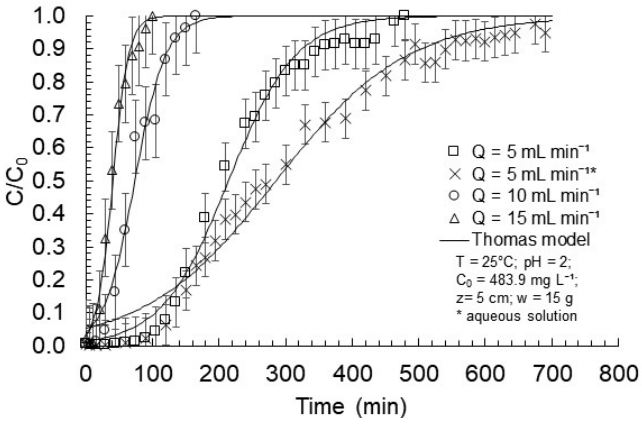

Fig. 5. Breakthrough curves of RhB adsorption (aqueous solution and real gemstones' wastewater treated by electro-Fenton) by strongly acid resin.

Table 4 shows the Thomas and Wolborska model parameters adjusted to the adsorption breakthrough curve of the 5, 10, and 15 mL min^{-1} flows, and the adsorption isotherms predicted values of the bed stoichiometric capacity. The determination coefficient (R^2), indicates that the Thomas model is able to predict the RhB adsorption in the dyeing wastewater of gemstones (solid lines in Fig. 5). The Thomas constant values (k_T) have increased with the flow, confirming that the mass transfer was faster with the flow increase. This occurs because the flow

increase reduces the mass transfer resistance between the wastewater ant the solid adsorbent [45,46].

The maximum adsorption capacity "q_0" predicted by Thomas model has decreased with the flow increase, and its values were inferior to the bed stoichiometric capacity (q_e) predicted by the equilibrium curve (Langmuir model). This difference, along with the low mass transfer coefficients, indicates that the resin saturation in the adsorption bed occurred superficially, and the values observed in the equilibrium tests were only possible due to the large contact time. The k_T values found were low, and had resulted in a maximum adsorption capacity smaller than q_e [47,48]. This difference might have been due to the low porosity of the studied adsorbent.

3.3. Characterization of electro-Fenton/adsorption obtained effluent

Fig. 6 shows the removal efficiencies of RhB, color, turbidity, and DOQ after each step of the process. It is possible to observe that the electro-Fenton process is suitable to partially remove the concentration of RhB, color, and COD. The non-proportional COD reduction relative to the RhB removal demonstrates that dye was partially mineralized during the electro-Fenton process. This behavior justifies the need to apply adsorption as a complementary treatment technique. In addition, RhB removal is close to the optimized value by the statistical model obtained by the response surface methodology. Moreover, the turbidity is completely reduced due to the cumulative effect of compound degradation and the flotation of suspended substances by the air bubbles and hydrogen generated in the electrolytic reactor.

Already, after adsorption on a bed of strong cationic resin is observed the complete removal of RhB. Using a bed 300 mm long it was possible to operate for 330 min (data not shown), obtaining removals of RhB higher than 99.5% in this interval. This value is similar to the color removal of agate dyeing effluents using sodium hypochlorite [2]. However, the authors report the presence of organochlorines due to incomplete dye mineralization. In addition, the adsorption system provided increased color removal (from 54% to 89%) and COD (from 50% to 68%). This suggests that RhB no-completely mineralized by the electro-Fenton process were removed during adsorption.

However, it should be noted that the final COD concentration was higher than 1,700 mg L^{-1}, which is about five times superior to the limit defined by local legislation for effluent emissions of this type of establishment [34]. Similar COD concentrations after the ozonization treatment of agate dyeing wastewater were observed by Machado et al. [49]. Sindelar et al. [50] observed a 62% reduction in the organic load and 20.5% of total nitrogen of agate dyeing wastewater using photodegradation and electrodialysis coupled processes. This value may be associated with other substances, including alcohol and detergents, used in the dyeing and washing of gemstones.

Machado et al. [49] suggest that other even more drastic oxidative methods be used for the complete reduction of COD in gemstones dyeing wastewater. However, given the absence of dye, turbidity, and low residual color, we believe that treated effluent can be reused in the agate processing such, for example, dyeing, cutting, or sanding stages.

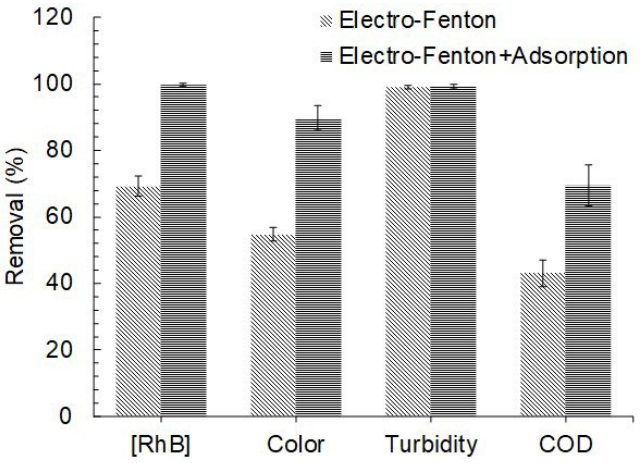

Fig. 6. Cumulative effect of electro-Fenton and adsorption process on the real gemstone's wastewater treatment.

4. Conclusion

In this work, it has been studied as an alternative method for the removal of RhB present in real effluents from the dyeing of semi-precious stones through electro-Fenton coupled to adsorption. We have found that the electro-Fenton process, although efficient in the removal of RhB, requires bigger time and a relatively expensive energy cost for the complete removal of the dye. However, if applied as a previous method of treatment can be promising, presenting costs in the order of 1.8 kWh per kg of removed RhB.

Subsequently, the adsorption was applied satisfactorily for the removal of the dye present in the effluent using a strong cation resin at pH 2.0. Under these conditions, the resin presented an adsorption capacity of RhB in the actual effluent of 247.3 mg g^{-1}. Adsorption isotherms were predicted by the Langmuir model. Fixed bed adsorption of RhB in real wastewater of gemstones dyeing were predicted by the Thomas model. The increase of flow rate causes an increase in mass transfer rates but a reduction in the stoichiometric capacity of the bed. Thus, with a flow rate of 5 mL min^{-1} the rupture time was 60 min.

The electro-Fenton process coupled with adsorption with strongly acidic resin was capable of removing more than 99.5% of RhB present in gemstones dyeing wastewater, being an effective conventional adsorbent for the complementary treatment of the dyeing process wastewater of gemstones.

Acknowledgments

The authors acknowledge the Gemstones and Jewelry Technology Center (CTPedras) for the technical support of the research. To De Nora Inc., (Brazil) for the Ti/RuO_2 anode supply. To the University of Passo Fundo for the scholarship and to National Council for Scientific and Technological Development (CNPQ) for the financial support to the research (Proc. 405311/2016–8).

Symbols

C_0 — Initial concentration in the liquid phase
CE — Energy cost of treatment
C_e — Equilibrium concentration at the liquid phase
C_f — Final concentration in the liquid phase
k_F — Constant of the Freundlich model
k_L — Constant of the Langmuir model
k_{Th} — Kinetic constant of the Thomas model
k_w — Kinetic constant of the Wolborska model
L — Bed length
LUB — Length of unused bed
n — Heterogeneity factor
Q — Flow rate
q_0 — Stoichiometric capacity of the bed
q_e — Adsorption capacity at equilibrium
q_m — Maximum adsorption capacity
R — Removal
R^2 — Determination coefficient
t — Operation time
t_b — Breakthrough time
t_e — Exhaustion time
V — Solution volume
V_b — Volume of treated effluent
v_z — Interstitial velocity
w — Adsorbent mass
z — Bed length

References

[1] F. Motahari, M.R. Mozdianfard, M. Salavati-Niasari, Synthesis and adsorption studies of NiO nanoparticles in the presence of H_2acacen ligand, for removing Rhodamine B in wastewater treatment, Process Saf. Environ. Prot., 93 (2015) 282–292.
[2] T.M. Pizzolato, E. Carissimi, E.L. Machado, I.A.H. Schneider, Colour removal with NaClO of dye wastewater from an agate-processing plant in Rio Grande do Sul, Brazil, Int. J. Miner. Process., 65 (2002) 203–211.
[3] F.S. Vilasbôas, C.R. Santos, I.A.H. Schneider, Environmental issues on the industrial processing of raw agate, Geomaterials, 7 (2017) 13–24.
[4] M. Danish, T. Ahmad, R. Hashim, N. Said, M.N. Akhtar, J. Mohamad-Saleh, O. Sulaiman, Comparison of surface properties of wood biomass activated carbons and their application against Rhodamine B and methylene blue dye, Surf. Interfaces, 11 (2018) 1–13.
[5] X. Chen, J. Dai, G. Shi, L. Li, G. Wang, H. Yang, Sonocatalytic degradation of Rhodamine B catalyzed by β–Bi_2O_3 particles under ultrasonic irradiation, Ultrason. Sonochem., 29 (2016) 172–177.
[6] J. Tian, J. Zhao, A.M. Olajuyin, M.M. Sharshar, T. Mu, M. Yang, J. Xing, Effective degradation of rhodamine B by electro-Fenton process, using ferromagnetic nanoparticles loaded on modified graphite felt electrode as reusable catalyst in neutral pH condition and without external aeration, Environ. Sci. Pollut. Res., 23 (2016) 15471–15482.
[7] M. Zhu, Y. Cai, S. Liu, M. Fang, M. Tan, X. Liu, M. Kong, W. Xu, H. Mei, T. Hayat, $K_2Ti_6O_{13}$ hybridized graphene oxide: effective enhancement in photodegradation of RhB and photoreduction of U(VI), Environ. Pollut., 248 (2019) 448–455.
[8] A. Ghaffar, X. Zhu, B. Chen, Biochar composite membrane for high performance pollutant management: fabrication, structural characteristics and synergistic mechanisms, Environ. Pollut., 233 (2018) 1013–1023.
[9] M. Goswami, P. Phukan, Enhanced adsorption of cationic dyes using sulfonic acid modified activated carbon, J. Environ. Chem. Eng., 5 (2017) 3508–3517.
[10] I. Sirés, E. Brillas, M.A. Oturan, M.A. Rodrigo, M. Panizza, Electrochemical advanced oxidation processes: today and tomorrow, A review, Environ. Sci. Pollut. Res., 21 (2014) 8336–8367.
[11] S. Qiu, D. He, J. Ma, T. Liu, T.D. Waite, Kinetic modeling of the electro-Fenton process: quantification of reactive oxygen species generation, Electrochim. Acta, 176 (2015) 51–58.
[12] P.V. Nidheesh, R. Gandhimathi, Electro Fenton oxidation for the removal of Rhodamine B from aqueous solution in a bubble column reactor under continuous mode, Desal. Water Treat., 55 (2014) 263–271.
[13] J. Meijide, S. Rodríguez, M.A. Sanromán, M. Pazos, Comprehensive solution for acetamiprid degradation: combined electro-Fenton and adsorption process, J. Electroanal. Chem., 808 (2018) 446–454.
[14] H. Roth, Y. Gendel, P. Buzatu, O. David, M. Wessling, Tubular carbon nanotube-based gas diffusion electrode removes persistent organic pollutants by a cyclic adsorption–electro-Fenton process, J. Hazard. Mater., 307 (2016) 1–6.
[15] H. Zhao, Q. Wang, Y. Chen, Q. Tian, G. Zhao, Efficient removal of dimethyl phthalate with activated iron-doped carbon aerogel through an integrated adsorption and electro-Fenton oxidation process, Carbon, 124 (2017) 111–122.
[16] E. Rosales, D. Anasie, M. Pazos, I. Lazar, M.A. Sanromán, Kaolinite adsorption-regeneration system for dyestuff treatment by Fenton based processes, Sci. Total Environ., 622–623 (2018) 556–562.
[17] H. Benchekor, A. Iddou, H. Hentit, A. Aziz, J.S. Piccin, Multilayer adsorption of purple NR5 industrial dye by *Aristeus antennautus* shell in aqueous solution, Key Eng. Mater., 762 (2018) 109–114.
[18] S. Kakkar, A. Malik, S. Gupta, Treatment of pulp and paper mill effluent using low cost adsorbents: an overview, J. Appl. Nat. Sci., 10 (2018) 695–704.
[19] C.S. Gomes, J.S. Piccin, M. Gutterres, Optimizing adsorption parameters in tannery-dye-containing effluent treatment with leather shaving waste, Process Saf. Environ. Prot., 99 (2016) 98–106.
[20] M.L.G. Vieira, M.S. Martinez, G.B. Santos, G.L. Dotto, L.A.A. Pinto, Azo dyes adsorption in fixed bed column packed with different deacetylation degrees chitosan coated glass beads, J. Environ. Chem. Eng., 6 (2018) 3233–3241.
[21] D.O. Cooney, Adsorption Design for Wastewater Treatment, CRC Press, Boca Raton, FL, 1998.
[22] APHA, Standard Methods for Examination of Water and Wastewater, 22nd ed., American Public Health Association, Washington, DC, 2014, p. 1360.
[23] D.C. Montgomery, Design and Analysis of Experiments, John Wiley & Sons, New Jersey, USA, 2017.
[24] M. Sun, Y. Liu, W. Xiang, L.-F. Zhai, Electricity-induced catalytic oxidation of RhB by O_2 at a graphite anode, Electrochim. Acta, 158 (2015) 314–320.
[25] J.T. Pizutti, R.C. Santos, M. Hemkemeier, J.S. Piccin, Electrocoagulation coupled adsorption for anaerobic wastewater post-treatment and reuse purposes, Desal. Water Treat., 160 (2019) 144–152.
[26] A. De Rossi, M.R. Rigon, M. Zaparoli, R.D. Braido, L.M. Colla, G.L. Dotto, J.S. Piccin, Chromium(VI) biosorption by *Saccharomyces cerevisiae* subjected to chemical and thermal treatments, Environ. Sci. Pollut. Res., 25 (2018) 19179–19186.
[27] J.S. Piccin, T.R.S. Cadaval, L.A.A. Pinto, G.L. Dotto, Adsorption Isotherms in Liquid Phase: Experimental, Modeling, and Interpretations, A. Bonilla-Petriciolet, D. Mendoza-Castillo, H. Reynel-Ávila, Eds., Adsorption Processes for Water Treatment and Purification, Springer, Cham, 2017, pp. 19–51.
[28] G.L. Dotto, N.P.G. Salau, J.S. Piccin, T.R.S. Cadaval, L.A.A. Pinto, Adsorption Kinetics in Liquid Phase: Modeling for Discontinuous and Continuous Systems, A. Bonilla-Petriciolet, D. Mendoza-Castillo, H. Reynel-Ávila, Eds., Adsorption Processes for Water Treatment and Purification, Springer, Cham, 2017, pp. 53–76.
[29] M. Zhou, Q. Yu, L. Lei, G. Barton, Electro-Fenton method for the removal of methyl red in an efficient electrochemical system, Sep. Purif. Technol., 57 (2007) 380–387.
[30] A. Özcan, Y. Şahin, A.S. Koparal, M.A. Oturan, Carbon sponge as a new cathode material for the electro-Fenton process:

comparison with carbon felt cathode and application to degradation of synthetic dye basic blue 3 in aqueous medium, J. Electroanal. Chem., 616 (2008) 71–78.
[31] I. Arslan-Alaton, G. Tureli, T. Olmez-Hanci, Treatment of azo dye production wastewaters using photo-Fenton-like advanced oxidation processes: optimization by response surface methodology, J. Photochem. Photobiol., A, 202 (2009) 142–153.
[32] P.V. Nidheesh, R. Gandhimathi, Trends in electro-Fenton process for water and wastewater treatment: an overview, Desalination, 299 (2012) 1–15.
[33] A.L. Barros, T.M. Pizzolato, E. Carissimi, I.A.H. Schneider, Decolorizing dye wastewater from the agate industry with Fenton oxidation process, Miner. Eng., 19 (2006) 87–90.
[34] State Council from the Environment, Resolution CONSEMA n° 355/2017, Provides the Criteria and Standards for Liquid Effluent Emission to Generator Sources that Release their Effluents in Surface Waters in the State of Rio Grande do Sul, 2017. Available at: https://www.sema.rs.gov.br/upload/arquivos/201707/19110149–355–2017-criterios-e-padroes-de-emissao-de-efluentes-liquidos.pdf (in Portuguese).
[35] S.M. Al-Rashed, A.A. Al-Gaid, Kinetic and thermodynamic studies on the adsorption behavior of Rhodamine B dye on Duolite C-20 resin, J. Saudi. Chem. Soc., 16 (2012) 209–215.
[36] Ö. Aydin, C. Özmetin, M. Korkmaz, B.A. Fil, A semiempirical kinetic model for removal of iron (Fe^{3+}) from saturated boric acid solution by ion exchange using amberlite IR-120 resin, Part. Sci. Technol., 35 (2017) 505–511.
[37] C.H. Giles, T.H. MacEwan, S.N. Nakhwa, D. Smith, Studies in adsorption. Part XI. A system of classification of solution adsorption isotherms, and its use in diagnosis of adsorption mechanisms and in measurement of specific surface areas of solids, J. Chem. Soc., (1960) 3973–3993, https://pubs.rsc.org/en/content/articlelanding/1960/jr/jr9600003973/unauth#!divAbstract.
[38] J.S. Piccin, C.S. Gomes, B. Mella, M. Gutterres, Color removal from real leather dyeing effluent using tannery waste as an adsorbent, J. Environ. Chem. Eng., 4 (2016) 1061–1067.
[39] M. Hadavifar, N. Bahramifar, H. Younesi, Q. Li, Adsorption of mercury ions from synthetic and real wastewater aqueous solution by functionalized multi-walled carbon nanotube with both amino and thiolated groups, Chem. Eng. J., 237 (2014) 217–228.
[40] J. Anandkumar, B. Mandal, Adsorption of chromium(VI) and Rhodamine B by surface modified tannery waste: kinetic, mechanistic and thermodynamic studies, J. Hazard. Mater., 186 (2011) 1088–1096.
[41] Y. Huang, X. Zheng, S. Feng, Z. Guo, S. Liang, Enhancement of rhodamine B removal by modifying activated carbon developed from *Lythrum salicaria* L. with pyruvic acid, Colloids Surf., A, 489 (2016) 154–162.
[42] T. Santhi, A.L. Prasad, S. Manonmani, A comparative study of microwave and chemically treated *Acacia nilotica* leaf as an eco friendly adsorbent for the removal of rhodamine B dye from aqueous solution, Arabian J. Chem., 7 (2014) 494–503.
[43] M.C. Bruzzoniti, M. Appendini, B. Onida, M. Castiglioni, M. Del Bubba, L. Vanzetti, P. Jana, G.D. Sorarú, L. Rivoira, Regenerable, innovative porous silicon-based polymer-derived ceramics for removal of methylene blue and rhodamine B from textile and environmental waters, Environ. Sci. Pollut. Res., 25 (2018) 10619–10629.
[44] A. Ghribi, M. Bagane, Removal of Rhodamine B from aqueous solution using natural clay by fixed bed column method, Int. J. Chem. Mol. Eng., 10 (2016) 94–97.
[45] A.M.D. Canteli, D. Carpiné, A.P. Scheer, M.R. Mafra, L. Igarashi-Mafra, Fixed-bed column adsorption of the coffee aroma compound benzaldehyde from aqueous solution onto granular activated carbon from coconut husk, LWT Food Sci. Technol., 59 (2014) 1025–1032.
[46] M.H. El-Naas, M.A. Alhaija, S. Al-Zuhair, Evaluation of an activated carbon packed bed for the adsorption of phenols from petroleum refinery wastewater, Environ. Sci. Pollut. Res., 24 (2017) 7511–7520.
[47] R. Han, Y. Wang, W. Zou, Y. Wang, J. Shi, Comparison of linear and nonlinear analysis in estimating the Thomas model parameters for methylene blue adsorption onto natural zeolite in fixed-bed column, J. Hazard. Mater., 145 (2007) 331–335.
[48] M.A. Mahmoud, Adsorption of U(VI) ions from aqueous solution using silicon dioxide nanopowder, J. Saudi Chem. Soc., 22 (2018) 229–238.
[49] E.L. Machado, V.S. Dambros, L.T. Kist, E.A.A. Lobo, S.B. Tedesco, C.C. Moro, Use of ozonization for the treatment of dye wastewaters containing Rhodamine B in the Agate Industry, Water Air Soil Pollut., 223 (2012) 1753–1764.
[50] F.W. Sindelar, L.F. Silva, V.R. Machado, L.C. Santos, S. Stülp, Treatment of effluent from the agate dyeing industry using photodegradation and electrodialysis processes, Sep. Sci. Technol., 50 (2015) 142–147.

Supplementary information

Supplementary material 1

Matlab routines for non-linear regression adsorption isotherms and breakthrough curves.

Supplementary material 2

Statistical analysis of central composite design applied to electro-Fenton process optimization.

Table S2.1
Analysis of variance of current density (X_1), pH (X_2), and Fe^{2+} concentration (X_3) on the RhB removal and energy consumption of electro-Fenton process

Effect	SS	DF	MS	*F*	*p*
		RhB removal (*R*)			
X_1 (*L*)	7.17	1	7.17	0.42	0.538
X_1^2 (*Q*)	3.19	1	3.19	0.19	0.679
X_2 (*L*)	280.94	1	280.94	16.40	0.005
X_2^2 (*Q*)	3.00	1	3.00	0.18	0.688
X_3 (*L*)	6.10	1	6.10	0.36	0.569
X_3^2 (*Q*)	2.37	1	2.37	0.14	0.721
$X_1 \times X_2$	2.29	1	2.29	0.13	0.726
$X_1 \times X_3$	7.94	1	7.94	0.46	0.518
$X_2 \times X_3$	<0.01	1	<0.01	<0.01	0.999
Error	119.89	7	17.13		
Total	435.82	16			
		Energy consumption (CE)			
X_1 (*L*)	13.89	1	13.89	45.33	0.000
X_1^2 (*Q*)	1.02	1	1.02	3.31	0.112
X_2 (*L*)	9.43	1	9.43	30.76	0.001
X_2^2 (*Q*)	0.57	1	0.57	1.85	0.215
X_3 (*L*)	0.00	1	0.00	0.00	0.967
X_3^2 (*Q*)	0.00	1	0.00	0.00	0.972
$X_1 \times X_2$	0.39	1	0.39	1.26	0.299
$X_1 \times X_3$	0.12	1	0.12	0.38	0.558
$X_2 \times X_3$	0.19	1	0.19	0.61	0.461
Error	2.15	7	0.31		
Total	27.56	16			

Table S2.2
Regression coefficients of significate variables on the RhB removal and energy consumption of electro-Fenton process

Parameter	Regression coefficients	Standard error	*t*	*p*	Confidence limit	
					+95%	–95%
RhB removal (*R*)						
Mean	57.65	0.78	74.0	0.000	55.99	59.32
X_2 (*L*)	–4.54	0.87	–5.2	0.000	–6.39	–2.68
Energy consumption (CE)						
Mean	2.85	0.20	14.0	0.000	2.40	3.30
X_1 (*L*)	1.01	0.13	7.9	0.000	0.73	1.29
X_1^2 (*Q*)	0.30	0.13	2.2	0.048	0.00	0.59
X_2 (*L*)	0.83	0.13	6.5	0.000	0.55	1.11
X_2^2 (*Q*)	0.22	0.13	1.7	0.125	–0.07	0.52
$X_1 \times X_2$	0.22	0.17	1.3	0.215	–0.15	0.59

Table S2.3
Quality and covariance analysis of predicted model for the RhB removal and energy consumption of electro-Fenton process

Effect	SS	DF	MS	*F*	*p*
RhB removal (*R*)					
Regression	56,790.1	2	28,395.0	2,750.1	<0.001
Residual	154.9	15	10.3		
Total	56,944.9	17			
Corrected total	435.8	16			
Regression vs. corrected	56,790.1	2	28,395.0	1,042.5	<0.001
R^2	0.644				
Adjusted R^2	0.621				
Energy consumption (*C*)					
Regression	206.8	6	34.5	154.9	<0.001
Residual	2.4	11	0.2		
Total	209.3	17			
Corrected total	27.6	16			
Regression vs. corrected	206.8	6	34.5	20.0	<0.001
R^2	0.911				
Adjusted R^2	0.871				

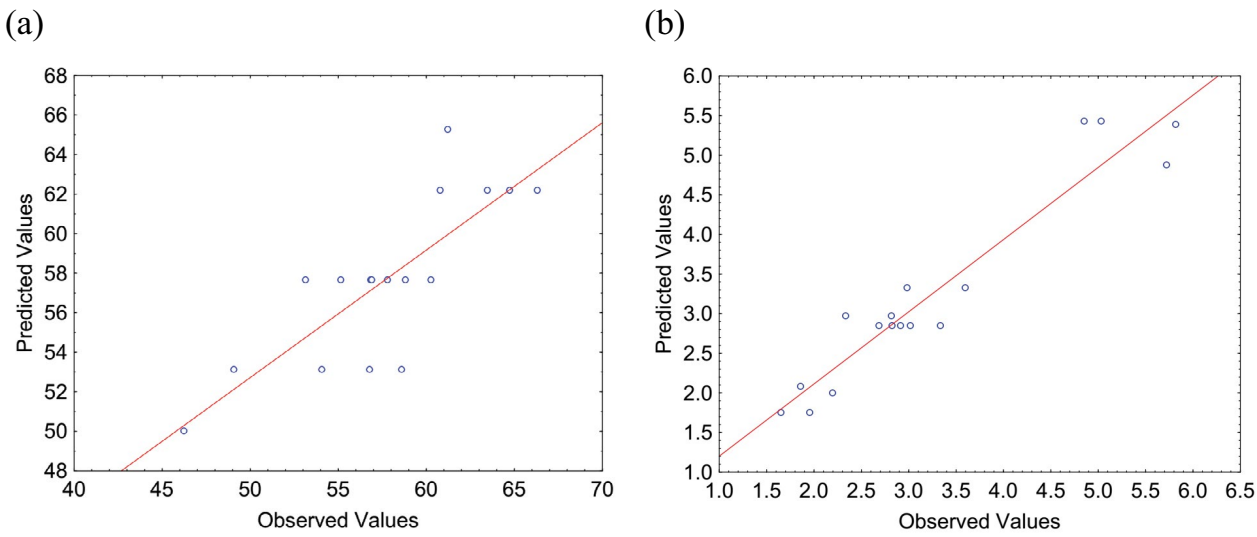

Fig. S2.1. Residual plots of observed and predict values of (a) RhB removal and (b) energy consumption.

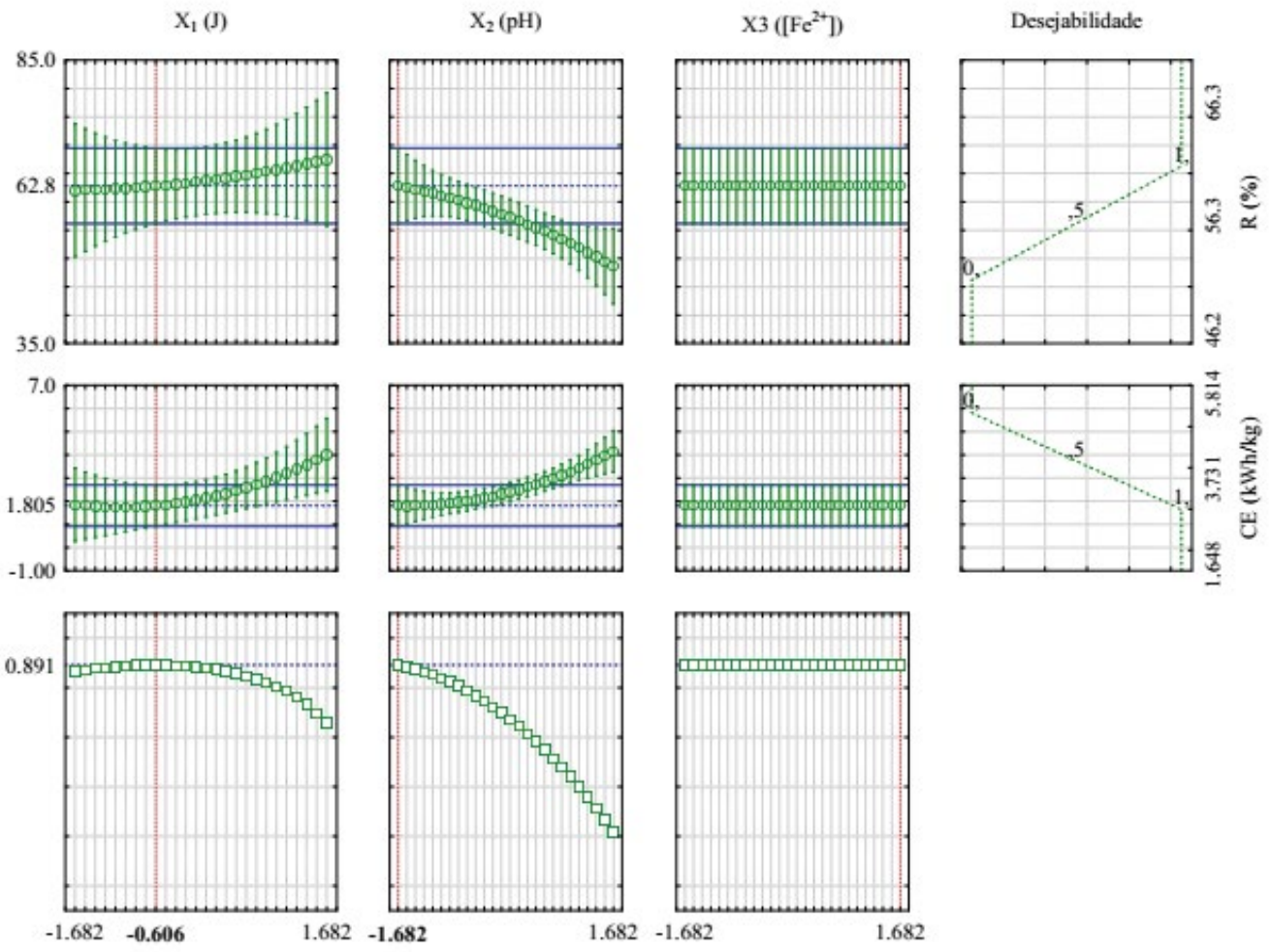

Fig. S2.1. Desirability profile for optimization of RhB removal (a) and energy consumption (b) of electro-Fenton process